Universiteit Utrecht

Faculteit Bètawetenschappen

Determining the radius of trapped gold nanoparticles with Mie scattering theory

Bachelor Thesis

S.D.C. Roscam Abbing

Study: Natuur- en Sterrekunde

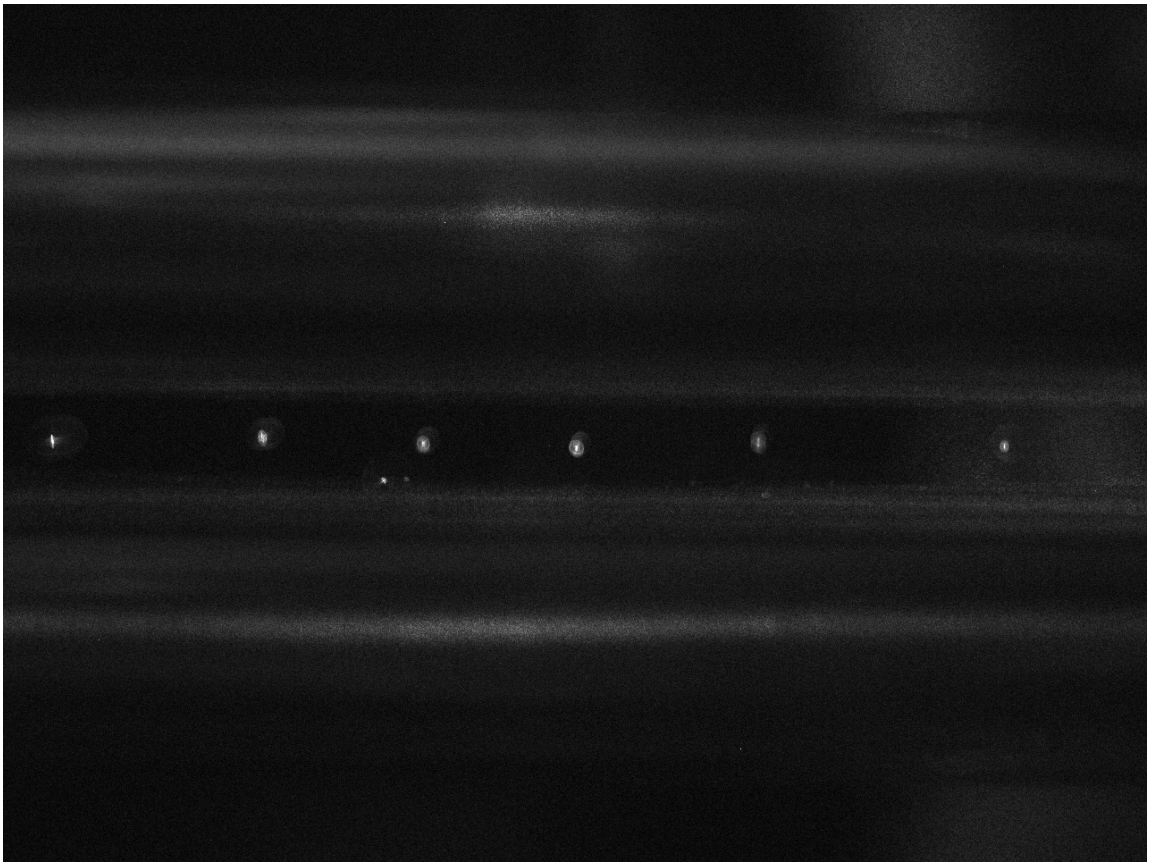

Supervisors:
Dr. D. van Oosten
M. Scholten, Msc
A. de Beurs, Bsc

June 2016

Abstract

For this research we trapped gold nanoparticles in a linear Paul trap. The nanoparticles were irradiated with a laser. The intensity of the sideways scattered light was measured for different polarization angles. We were able to determine the size of the trapped particles by making use of simulations, which are based on Mie theory. The radius of the trapped particles varies around 440 nm and 850 nm. The gold particles that are used for trapping have a diameter of 100 nm. This means the particles are aggregated once trapped.

Contents

1 Introduction

The interaction of light with nanoparticles displays several phenomena. If a laser is focused on a particle the light will be scattered. The way the light is scattered depends on the shape and the size of the particle it irradiates. It also depends on the wavelength of the light itself. The scattered light obtains information about the particle. Using the scattering properties of light information about the particle can be retreived.

It is also possible that the laser is so strong that the particle it irradiates evaporates, this is called laser ablation. Not everything about this process is known, so more research on the properties of nanoparticles in this process is necessary. For this it would be useful to research laser ablation on a single particle in free space. To realise this we need an environment for the particle where it is not affected by external factors. This environment can be created by a vacuum chamber. To make sure the particle is located in free space it is trapped with electric fields in the vacuum chamber. It was 1989 when Norman F. Ramsey, Hans G. Dehmelt and Wolfgang Paul won the Nobelprize in physics partly for their work on "*the development of the ion trap technique*" [1]. Paul used dynamic electric fields to create a quadruple ion trap, now known as the Paul trap [2]. With a Paul trap a charged particle can be trapped with electric fields.

The particles that are used for this experiment have a diameter of 100 nm. During the process of trapping the particles can form aggregates. For future research we want to examine single particles, therefore we want to know if the trapped particles are aggregated or not. The purpose of this research is to determine the size of the particles that are trapped in the linear Paul trap. To achieve this the particles are irradiated with a laser. When the laser is not strong enough to make the trapped particles evaporate, and under the assumption that the particles are spherical, the light will be scattered according to Mie theory. In 1908, Mie published a solution of Maxwell's equations. With this solution it was possible to describe the scattering of light on spherical particles of arbitrary size [3].

The theory of the Paul trap will be explained on the basis of the article "*Electromagnetic traps for charged and neutral particles*", written by Paul in 1990. Afterwards the Mie theory and the simulations that we used for this reserach will be presented. A description of the experimental setup and the way the experiment was executed follows in the next sections. The conclusion and the results are the final sections.

2 Theory

2.1 2D Paul trap

The motion of a mass on the end of a spring is described with Hookes Law. If a mass is moved away from its equilibrium point a linear force F pushes it back to its equilibirum, $F = -cx$, where c is a constant and x is the distance between the particle and the equilibirum point [2]. This movement is also called the classic harmonic oscillator. If the force F acts also in the y and z direction the mass has a parabolic shaped potential energy

$$U(x, y, z) = (\alpha x^2 + \beta y^2 + \gamma z^2), \tag{1}$$

where α, β and γ are constants. For this research it is desired that charged particles are trapped in free space. To bind a charged particle to a equilibrium point without using springs, electric fields can be used. The potential of the electric quadrupole field has the same shape as the potential energy of a mass on the end of a spring

$$\Phi(x, y, z) = \frac{\Phi_0}{2r_0^2}(\alpha x^2 + \beta y^2 + \gamma z^2), \tag{2}$$

where Φ_0 is the electric potential applied to the trap and r_0 is a size parameter which ensures that distance cancels out in the potential. Because we now use electric fields, we have to make sure the electric potential satisfies Laplace's equation. From Laplace's equation, $\Delta\Phi = 0$, it follows that $\alpha+\beta+\gamma = 0$. For instance this can be solved by setting $\alpha = 1 = -\gamma$, and $\beta = 0$, which results in a two-dimensional potential of the electric field.

$$\Phi = \frac{\Phi_0}{2r_0^2}(x^2 - z^2). \tag{3}$$

This potential can be produced by aligning four cylindrical rods in the y direction, as shown in Fig. 1. The center of the trap lies on the y axis. If a voltage of Φ_0 is applied to the electrodes, each electrode has a potential of $\pm\frac{\Phi_0}{2}$. This induces an electric field, where r_0 is defined as half the distance between two rods lying opposite to each other,

$$E_x = -\frac{\Phi_0}{r_0^2}x, \qquad E_z = \frac{\Phi_0}{r_0^2}z, \qquad E_y = 0. \tag{4}$$

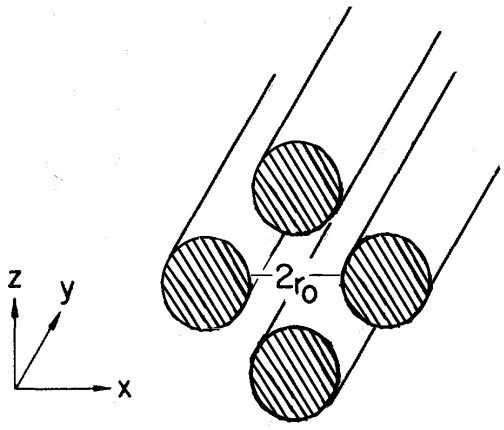

Figure 1: Schematic drawing of the linear Paul trap, consisting out of four rods. Opposite lying rods are separated by 2 r_0.

The constant voltage Φ_0 makes a particle, that is injected in the y direction, oscillate harmonically in the x-y plane. However the electric field in the z direction attracts the particle and therefore the movement of the particle in the z direction will increase exponentially in time. At a given moment the deflection of the particle will be too big and the particle leaves the trap. A solution is to alternate the sign of the electric forces in time, to keep the particles trapped in the center of the trap. Using a periodically oscillating voltage will solve this issue, it has the following shape

$$\Phi_0 = U + V\cos\omega t, \tag{5}$$

where U is a DC voltage, V is a RF voltage and ω is the driving frequency. If this voltage is applied the particles will move according to the following equations of motion,

$$\ddot{x} + \frac{e}{mr_0^2}(U + V\cos\omega t)x = 0, \qquad \ddot{z} - \frac{e}{mr_0^2}(U + V\cos\omega t)z = 0. \tag{6}$$

where e is the elementary charge, m the mass of the particle and x and z are parameters that define the position of the particle. If the quadrupole field was homogeneous, the time-dependent term in the equations above would cancel out in time. The particles couldn't be trapped in that case. But the quadrupole field is inhomogeneous so a small average force will always be directed towards the y axis. The particles therefore have a stable motion around the y axis. The differential equations that are used to describe the motions of the particles have the same shape as the Mathieu equations, written in dimensionless parameters.

$$\frac{d^2x}{d\tau^2} + (a + 2q\cos 2\tau)x = 0, \qquad \frac{d^2z}{d\tau^2} - (a + 2q\cos 2\tau)z = 0. \tag{7}$$

By comparing these equations to the equations of motion a, q and τ can be determined.

$$a = \frac{4eU}{mr_0^2\omega^2}, \qquad q = \frac{2eV}{mr_0^2\omega^2}, \qquad \tau = \frac{\omega t}{2}. \tag{8}$$

Whether the particles are stable around the y axis depends on the parameters a and q. In Fig. 2 we can observe the regions where the particles are stable and unstable. The Mathieu equations have a well known general derivation [4], but this derivation lies outside the scope of this research project.

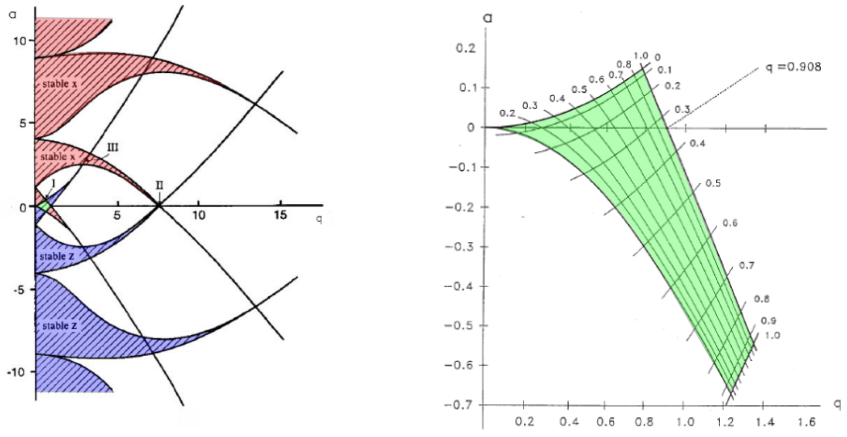

Figure 2: The red areas of the figure on the left represent the regions where the particle is stable in the x direction. The blue areas show the regions where the particle is stable in the z direction. This stability depends on the dimensionless parameters a and q, which are defined in Eq.8. The green area, near the origin, represents the parameter space where the particle is stable in both the x and z direction. This region is enlarged in the right figure. The values for a and q will be chosen from the green area. With these values the particles can be trapped [5].

2.2 Mie scattering

In this section the theory of Mie will be explained [6]. Afterwards the simulation that is used for this research project will be discussed.

2.2.1 Electromagnetic properties of light

Light is an electromagnetic wave. The way light is scattered by a particle depends on the shape of that particle [7]. It also depends on how the light is polarized. Light can be described by the Maxwell equations

$$\nabla \cdot \mathbf{D} = \rho_F, \tag{9}$$

$$\nabla \times \mathbf{E} + \frac{\delta \mathbf{B}}{\delta t} = 0, \tag{10}$$

$$\nabla \cdot \mathbf{B} = 0, \tag{11}$$

$$\nabla \times \mathbf{H} = \mathbf{J}_F + \frac{\delta \mathbf{D}}{\delta t} = 0, \tag{12}$$

where $\mathbf{E}$ is the electric field, $\mathbf{B}$ the magnetic field, ρ_F the free charge density and $\mathbf{J}_F$ the free current density. The electric displacement field $\mathbf{D}$ and the magnetizing field $\mathbf{H}$ are defined by

$$\mathbf{D} = \epsilon_0 \mathbf{E} + \mathbf{P}, \tag{13}$$

$$\mathbf{H} = \frac{\mathbf{B}}{\mu_0} - \mathbf{M}. \tag{14}$$

Here $\mathbf{P}$ is the electric polarization and $\mathbf{M}$ the magnetization, ϵ_0 the permittivity and μ_0 the permeability of free space. By using the Maxwell equations we derive that $\mathbf{E}$ and $\mathbf{H}$ satisfy the vector wave equation. This wave equation is valid in a linear, isotropic and homogeneous medium

$$\nabla^2 \mathbf{E} + k^2 \mathbf{E} = 0, \qquad \nabla^2 \mathbf{H} + k^2 \mathbf{H} = 0. \tag{15}$$

where k is the wave number appropriate to the surrounding medium. The wave number is defined as $\frac{2\pi}{\lambda}$, where λ is the wavelength of the light. Knowing that $\mathbf{E}$ and $\mathbf{H}$ must satisfy the vector wave equation, a solution for this equation can be found. In this research project the interest lies in how light is scattered by a spherical particle. This phenomena can be described by the vector spherical harmonics of the plane wave that is used and the cross sections of the scattered light [6]. The incident beam is a linear polarized plane wave. It can be written in spherical coordinates.

$$\mathbf{E}_i = E_0 e^{ikr\cos\theta} \hat{\mathbf{e}}_x, \tag{16}$$

where

$$\hat{\mathbf{e}}_x = \sin\theta\cos\phi\hat{\mathbf{e}}_r + \cos\theta\cos\phi\hat{\mathbf{e}}_\theta - \sin\phi\hat{\mathbf{e}}_\phi, \tag{17}$$

This will result in the following incident plane wave.

$$\mathbf{E}_i = E_0 e^{ikr\cos\theta}(\sin\theta\cos\phi\hat{\mathbf{e}}_r + \cos\theta\cos\phi\hat{\mathbf{e}}_\theta - \sin\phi\hat{\mathbf{e}}_\phi,), \tag{18}$$

where E_0 is the amplitude of the incident field. The angles θ and ϕ are explained in Fig. 3.

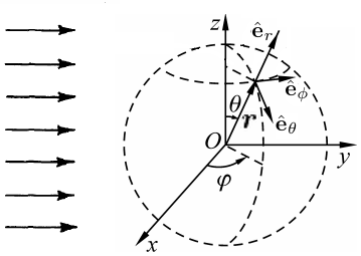

Figure 3: This figure shows a spherical particle in a spherical coordinate system. The arrows on the left side represent the incident beam. r is the position vector, θ is the polar angle and ϕ is the azimuth angle.

After rewriting the identity in Eq.16, the following expansion of the plane wave in vector harmonics can be derived.

$$\mathbf{E}_i = E_0 \sum_{n=1}^{\infty} i^n \frac{2n+1}{n(n+1)} (\mathbf{M}_{oln}^{(1)} - i\mathbf{N}_{eln}^{(1)}), \tag{19}$$

where $\mathbf{M}_{oln}^{(1)}$ and $\mathbf{N}_{eln}^{(1)}$ are vector harmonics of the first order [6]. The next step is to compute a similar expression for the scattered field. This can be achieved by multiplying the vector harmonics $\mathbf{M}_{oln}^{(1)}$ and $\mathbf{N}_{eln}^{(1)}$ with the scattering coefficients a_n and b_n.

$$\mathbf{E}_s = E_0 \sum_{n=1}^{\infty} i^n \frac{2n+1}{n(n+1)} (ia_n\mathbf{N}_{eln}^{(3)} - b_n\mathbf{M}_{oln}^{(3)}), \tag{20}$$

where $\mathbf{M}_{oln}^{(3)}$ and $\mathbf{N}_{eln}^{(3)}$ are vector harmonics of the third kind. These vector harmonics have angular eigenfunctions that can be substituted in Eq. 20 to simplify the formula and to clarify the angular dependency of the scattered light. This will emerge in the following subsection.

2.2.2 Mie scattering theory

To compute the scattered field the amplitude scattering matrix is used, which relates the incident field with the scattered field,

$$\begin{pmatrix} \mathbf{E}_{\parallel,s} \\ \mathbf{E}_{\perp,s} \end{pmatrix} = \frac{e^{ik(r-z)}}{-ikr} \begin{pmatrix} S_2 & S_3 \\ S_4 & S_1 \end{pmatrix} \begin{pmatrix} \mathbf{E}_{\parallel,i} \\ \mathbf{E}_{\perp,i} \end{pmatrix}. \tag{21}$$

where $\mathbf{E}_{\parallel,s}$ is the component of the electric field that is orientated parallel to the scattering plane (x-y plane), see Fig. 3. $\mathbf{E}_{\perp,s}$ is the component of the electric field that is orientated perpendicular to the scattering plane (z-y plane). $S_i (i = 1, 2, 3, 4)$ are the elements of the amplitude scattering matrix that depend on θ and ϕ. In the case of a spherical particle the elements S_3 and S_4 are 0, because of symmetry. This will result in the following amplitude scattering relations

$$\begin{pmatrix} \mathbf{E}_{\parallel,s} \\ \mathbf{E}_{\perp,s} \end{pmatrix} = \frac{e^{ik(r-z)}}{-ikr} \begin{pmatrix} S_2 \\ S_1 \end{pmatrix} \begin{pmatrix} \mathbf{E}_{\parallel,i} \\ \mathbf{E}_{\perp,i} \end{pmatrix}. \tag{22}$$

Where the elements S_1 and S_2 are defined as follows

$$S_1 = \sum \frac{2n+1}{n(n+1)} (a_n\pi_n + b_n\tau_n), \qquad S_2 = \sum \frac{2n+1}{n(n+1)} (a_n\tau_n + b_n\pi_n). \tag{23}$$

Here a_n and b_n are the scattering coefficients and π_n and τ_n are the angle-dependent functions. For this research a simulation is used where these coefficients are calculated numerically. To change the orientation of the light from parallel to perpendicular the light is rotated with 90° in the x-z plane. Recall that the parallel component is x-polarized light and the perpendicular component is z-polarized.

$$\mathbf{E}_{\parallel,s}(\phi; x\text{-polarized}) = \mathbf{E}_{\perp,s}(\phi + \frac{\pi}{2}; z\text{-polarized}). \tag{24}$$

2.2.3 Mie scattering simulation

According to Bohren and Huffmann "*Although the formal solution for this problem has been available for many years, only since the advent of large digital computers has it been a practical means for detailed computations*". This section will describe Mie theory on the basis of simulations. The package that is used for this research project is called Pymiecoated [8]. With this package the scattering coefficients and the angle-dependent functions can be calculated. As a result, also S_1 and S_2 can be calculated. Pymiecoated is also used to calculate the visibility v of a particle. The visiblity is the ratio of the difference between the intensity of parallel and perpendicular scattered light and the total intensity of parallel and perpendicular light.

$$v = \frac{|\mathbf{E}_{\parallel}|^2 - |\mathbf{E}_{\perp}|^2}{|\mathbf{E}_{\parallel}|^2 + |\mathbf{E}_{\perp}|^2}. \tag{25}$$

Combining Eq. 25 with Eq. 22, the visiblity can be rewritten in terms of the amplitude scattering elements S_1 and S_2

$$v = \frac{|S_2|^2 - |S_1|^2}{|S_2|^2 + |S_1|^2}. \tag{26}$$

This formula is used to create Fig. 4, where the dependency on the size of the particle for two different wavelengths of the incident beam is shown. The y axis represents the visibility, which lies between -1 and 1. On the x axis the radius of the particle is plotted, see Fig. 4. The black line represents a fictional visibility of -0.8, that could be measured with a laser with a wavelength of 633 nm. The red line represents the visibility calculated for a laser with a wavelength of 633 nm. There are multiple intersections of the black and the red line, which means there are several values for the particle size possible. To determine the size of a particle, values for the visibility for at least two wavelengths are needed. The blue line represents a fictional visibility of 0.3, that could be measured with a laser with a wavelength of 543 nm. The green line represents the visibility calculated for a laser with a wavelength of 535 nm. In Fig. 4, both wavelenghts are shown.

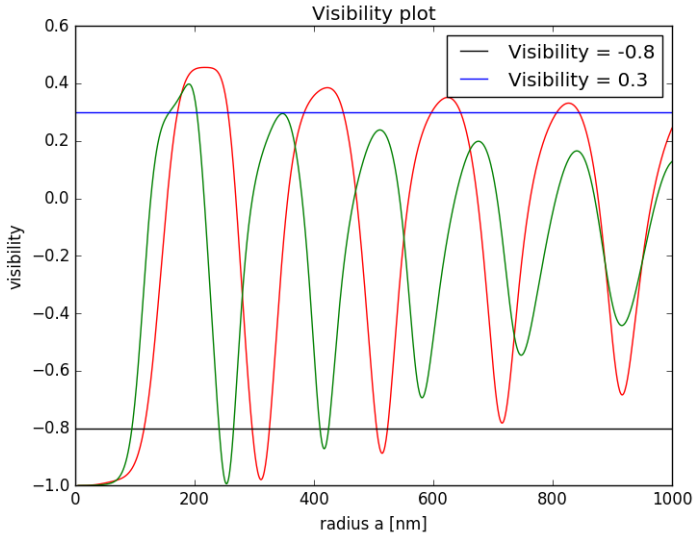

Figure 4: Simulation of the visibility plotted against the radius of the particle in nm. The green line displays the wavelength $\lambda = 543$ nm, the red line that of $\lambda = 633$ nm. The black line represents a possible measurement with a laser with a wavelength of $\lambda = 633$ nm. The blue line represents a possible measurement with a laser with a wavelength of $\lambda = 543$ nm.

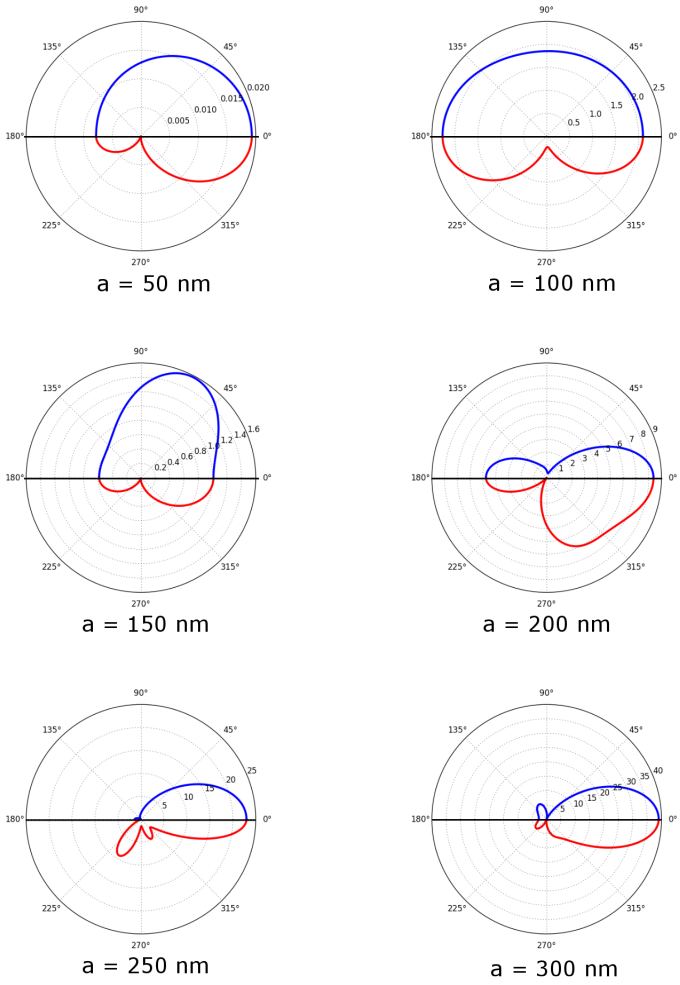

Figure 5: In this figure the scattering cross section for particles of different sizes is plotted. On the r axis the intensity of the scattered light is displayed. The blue line represents the perpendicular scattered light and the red line the parallel scattered light.

Another property that is simulated is the angular dependence of the scattered intensity of a spherical particle, shown in Fig. 5. Both the parallel as well as the perpendicular component are calculated making use of the amplitude scattering elements S_1 and S_2.

$$I_{\perp,s} = |S_1|^2, \qquad I_{\parallel,s} = |S_2|^2. \tag{27}$$

The figures show that for different sizes of the particles the light is scattered in different directions and amounts. The bigger the radius gets, the higher the intensity of the forward scattered light.

3 Experimental setup

This section contains information about the experimental setup that was built for this experiment. In Fig. 6, the entire experimental setup is presented. In Fig. 7, the Paul trap is shown.

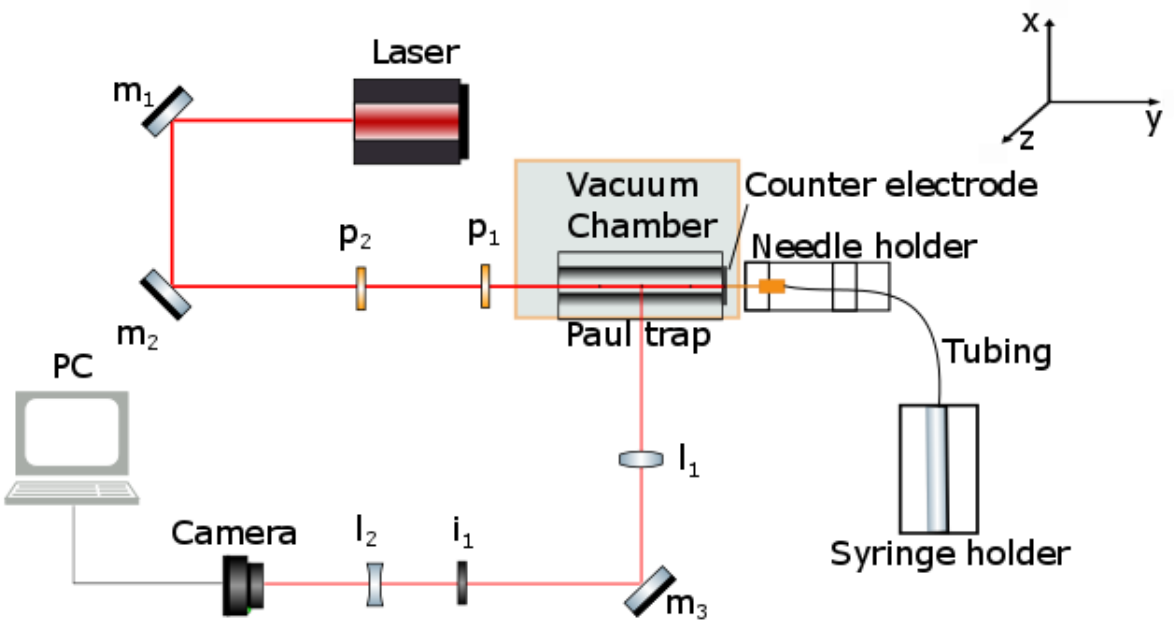

Figure 6: Top view of the experimental setup. The Paul trap is displayed in the middle, the red line represents the laser beam. m_1, m_2 and m_3 represent mirrors, p_1 and p_2 are polarizers. l_1 and l_2 are lenses and i_1 is an iris.

The particles that are used to trap in this experiment are gold nano colloids with a 100 nm diameter. They are stabilized in a solution of water with polyvinylpyrrolidone(PVP), which makes the particles negatively charged. To reduce the surface tension of the solution it is one in ten diluted with ethanol. The solution is injected into the trap with a syringe that is pushed by a micrometer screw, in order to ensure a constant flow. The fluid first passes a filter that filters most of the particles bigger than 220 nm. Tubing with an inner diameter of 100 μm made of Fused-Silica transports the fluid from the syringe to the needle. The needle has an inner diameter of 50 μm and is mounted onto a brass block. The tip of the needle is coated with a conductive coating.

The Paul trap consist out of four metal rods with each a diameter of 6mm. They have a spacing of 2 mm, see Fig. 7. The frequency and the voltage of the trap can be adjusted. A counter electrode is positioned at the front of the Paul trap. A high voltage of 2 kV is applied between the coated needle and the counter electrode. Because of the high potential the particles are repelled by the needle and they first form droplets at the tip of the needle. Little droplets with the colloids inside are accelerated towards the trap, this process is called electrospray. How high the voltage needs to be depends mostly on the distance between the needle and the counter electrode.

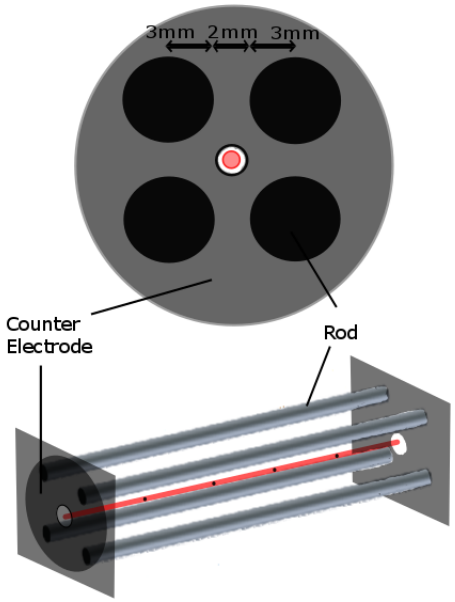

Figure 7: Schematic drawing of the Paul trap. The front is enlarged in the upper part of the figure. The rods have a radius of 3 mm and have a spacing of 2 mm.

Once the particles enter the trap they will stabilize in a one dimensional formation in the y direction, see Fig. 6 for the definition of the axes. The particles were trapped with $U = 690$ V and $f = 7$ kHz. The Paul trap is located in a vacuum chamber to make sure the stability of the colloids is not affected by the motion of air or other particles. The chamber is opened to inject the particles. Once the particles are stabilized in the trap the chamber is closed. A vacuum is applied slowly to not disturb the particles. The final pressure in the chamber lies between 12 Pa and 14 Pa.

For this experiment a Helium-Neon laser is used ($\lambda = 633$ nm). The laser beam is directed into the y axis, where the particles are located. Before the laser beam enters the trap it is polarized. A polarizer is used to filter out circular polarized components of the beam. Afterwards it passes a $\frac{1}{2}\lambda$ waveplate, to polarize the beam for a certain angle. The waveplate can be rotated in the x-z plane to rotate the polarization of the beam during the experiment.

The light that is scattered by the particles in the x-direction is imaged with a PointGrey Grasshopper3 camera. Both lenses, $\mathrm{l}_1(f = 180$ mm) and $\mathrm{l}_2(f = 50$ mm) are used to magnify the image. To reduce the background on the image an iris i_1 was used.

4 Results

For this research we analyzed five particles. The first step was to take pictures of these five particles. A colourmap was made of these pictures to define the location of the particles, see Fig. 8. For every picture the pixel values were summed up in the vertical direction. With these values a horizontal intensity plot was made for the five particles, see Fig. 9. The positions of the particles are denoteded by the arrows. The five particles are analysed separately. For each particle a region of interest was defined. This region is around 8 pixels in the vertical direction and 80 pixels in the horizontal direction around the particle.

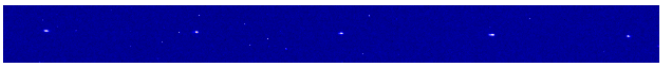

Figure 8: Colourmap image of the five particles. The particles are numbered from one to five, where the left particle is particle number one and the right particle is number five.

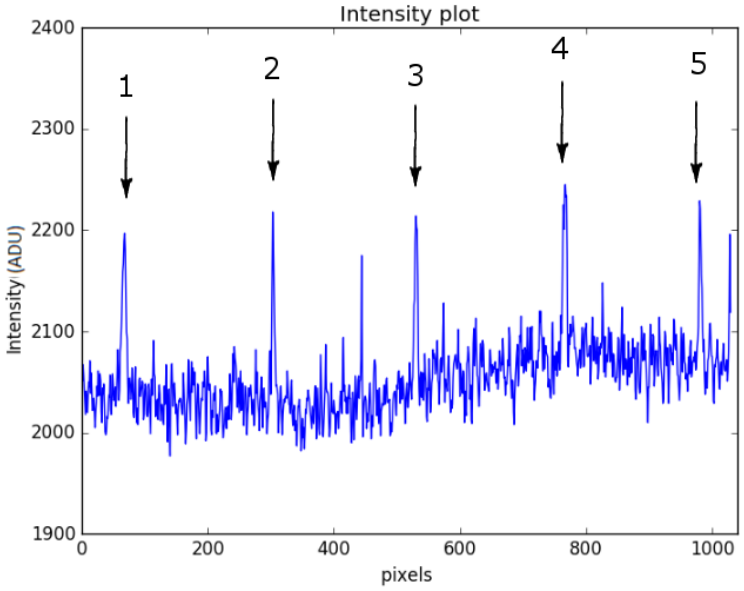

Figure 9: Intensity plot of Fig. 8. The pixels are summed up in the vertical direction. There are five peaks at the positions where the particles are visible denoted with arrows. The horizontal axis displays the pixel number in the horizontal direction of Fig. 8. The vertical axis displays the vertically summed up intensity.

Pictures were made for 37 different polarization angles, ranging from 0 to 180 degrees. The polarisation degree was changed in steps of 5 degrees each. For each separate orientation there were 100 pictures taken. An intensity plot was made from every picture, like Fig. 9. To calculate the intensity of the sideways scattered light of a particle a gaussian function was fitted to each of these intensity plots. The area under the gaussian was averaged for all pictures. The intensity of the sideways scattered light was determined for every polarisation angle separately.

The power of the laser fluctuated during the experiment. For every polarization angle the power was measured. The data was scaled to the fluctuations in the power of the laser. A sine function was fitted to these data points. This is done for every particle separately. This measurement was executed for two different wavelengths. For both wavelengths the visibility is calculated for each of the five particles. The data from these two wavelengths is presented in the following subsections.

4.1 Helium-Neon laser

The first measurement was done with a Helium-Neon laser ($\lambda = 633$ nm). The data of a typical particle is presented in this section, that is for particle number three, see Fig. 9 for the definition of particle three. The scattering amplitude of the sideways scattered light is plotted for each polarization angle, see Fig. 10. The data from the other four particles looks similar and can be found in the Appendix.

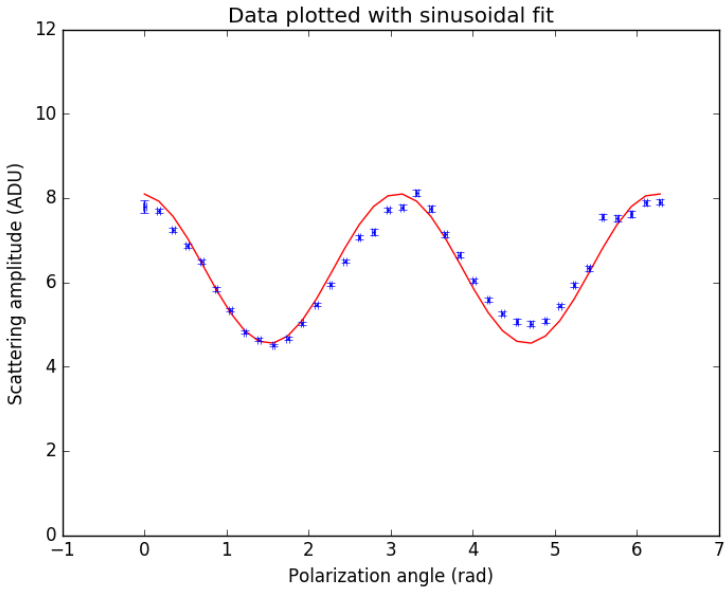

Figure 10: The blue dots represent the scattering amplitude that is calculated for particle three. The red line is the sine fit to these data points. The vertical axis displays the scattering amplitude of the sideways scattered light. The horizontal axis displays the polarization angle in radians.

To calculate the visibility the parallel and the perpendicular component of the electric field should be known, see Eq. 25. The maximum value for the scattering amplitude represents the parallel component. For a polarization angle of 0 radians the parallel component of the light was measured. The minimum value of the scattering amplitude represents the perpendicular component. Both the value of the parallel and the perpendicular component are calculated with the sine fit. In this case the parallel component was measured first and the sine function displays a maximum first. The visibility that is calculated for the third particle is 0.280 ± 0.006, see Fig. 11. For this visibility there are multiple intersections with the red line. That means there are several particle sizes which result in this visibility. These particle sizes are presented in Tab. 1.

Intersection #	Particle three
1	a = 165.3 ± 0.5 nm
2	a = 253.0 ± 0.4 nm
3	a = 376.6 ± 1. nm
4	a = 448.0 ± 0.7 nm
5	a = 589.0 ± 0.3 nm
6	a = 646.2 ± 0.9 nm
7	a = 800.0 ± 0.6 nm
8	a = 846.4 ± 1.2 nm

Table 1: For the first eight intersection points the radius that follows from the intersection is presented.

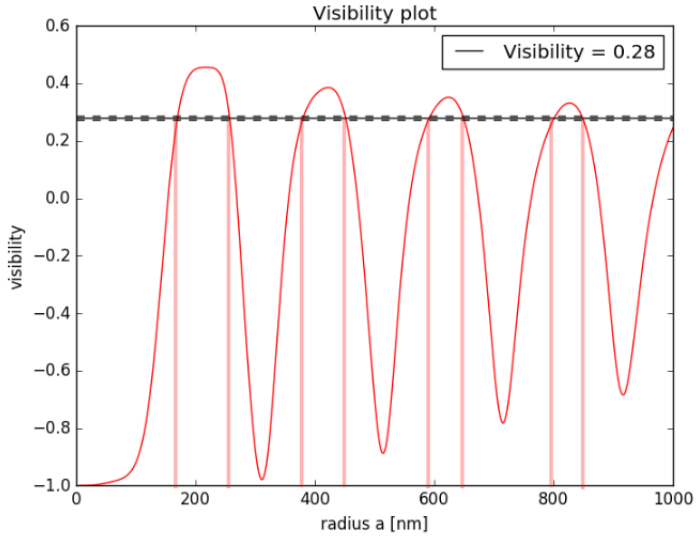

Figure 11: Visibility plot for particle three. The black line represents the measured visibility. The black dashed lines represents the standard deviation in the visibility. The red line is the simulation of the visibility for different particle sizes. The light red vertical lines are drawn to clarify the intersection points and the radius that follows from these intersections. On the horizontal axis the radius is given in nm. The vertical axis represents the visibility.

Each radius that follows from an intersection is still equally likely. Therefore we need either another value for the visibility for another wavelength, or we need another kind of analysis. Both options are executed, but the second option will be presented first. This option is based on something that was also noticed during this experiment, the amount of forward and sideway scattered light of the particles. This was observed but not quantified. A scattering plot is made for each radius that is found. These figures presents how a spherical particle of a particular size scatters light in the parallel and perpendicular direction, see Fig. 13. The angle at which the particles were observed from the frontal direction was around 20 degrees, see Fig. 12. In each of the scattering plots in Fig. 13 this angle is represented by the black oblique lines. The amplitude of the sideway scattered light can be seen for 90 degrees or 270 degrees. We observed that for the angle of 20 degrees the particles were still very visible. For an angle of 90 or 270 degrees the particles were very hard te see. The ratio between forward and sideway scattered light is therefore big. For the smaller particles we can observe from the figures that this ratio is small. This means that it is unlikely that the trapped particles have a radius of 165 nm or 253 nm. For the other possible particle sizes there is almost exclusively forward scattering. The intensity of the observed forward scattered light did not change a lot under smaller angles. Therefore the other particle sizes that are found are equally likely, based on this analysis.

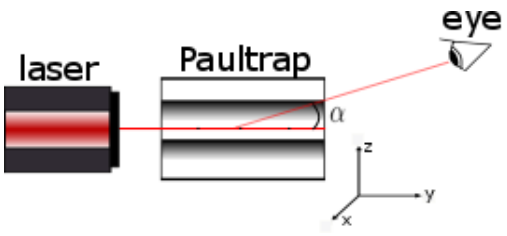

Figure 12: Sideview of the Paul trap. The forward scattered light can be viewed under an angle of around 20° degrees, α. It was not possible to observe the particles under a bigger angle because of the geometry of the vacuum chamber.

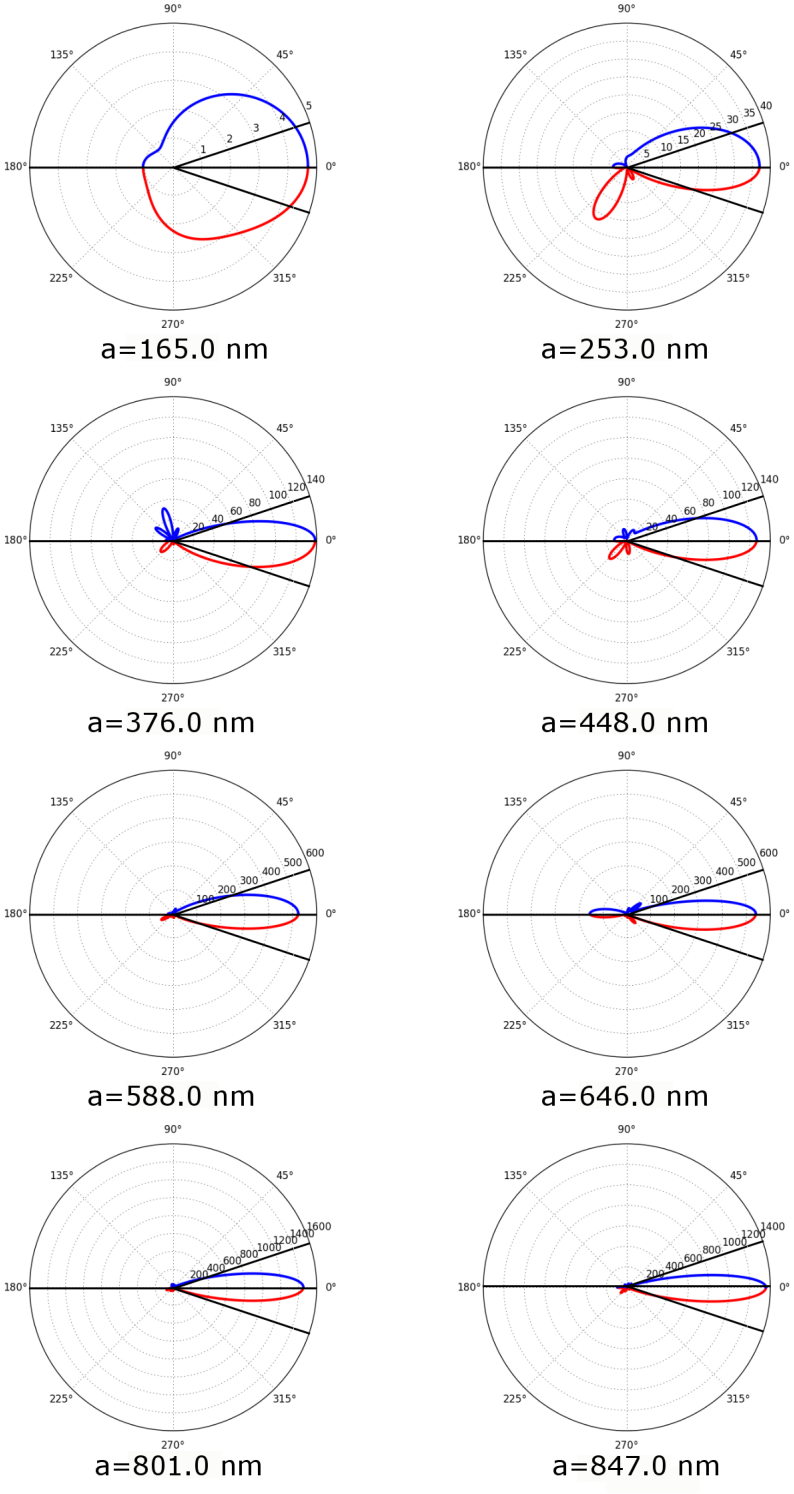

Figure 13: Simulation of the scattering of eight possible particles sizes for particle three, measured for the Helium-Neon laser. In each graph the parallel (blue) and perpendicular (red) component are shown. Here 0° degrees represents the forward direction, 180° the backward direction. In the r-axis the scattering amplitude is displayed. The two black oblique lines represent an angle of 20 degrees. For more information about how this figure was established, see Fig. 5.

4.2 Diode laser

The second measurement was done with a diode laser ($\lambda = 785$ nm). Only the results for the third particle are presented. The data from the other four particles can be found in the Appendix. The analysis for this measurement was done in the same way as for the Helium-Neon laser. For every polarization angle the intensity is plotted, see Fig. 14.

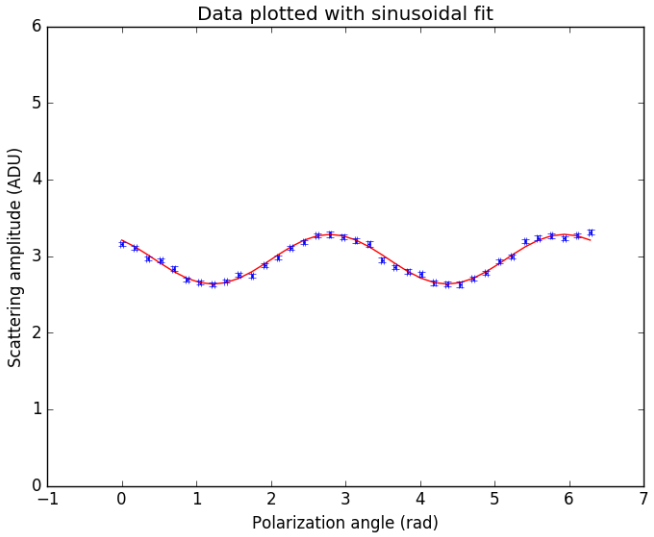

Figure 14: The blue dots represent the scattering amplitude calculated with the gaussian fit from the pictures for particle three. The red line is the sine fit to these data points. On the horizontal axis the polarization angle is displayed in radians. The vertical axis represents the scattering amplitude in analog to digital units.

At this measurement the perpendicular component of the scattered light was measured for a polarization angle of 0 radians. From Fig. 14 it can be seen that the sine fit displays a maximum at an angle of 0 radians. Therefore the maximum value of the sine represents the perpendicular component. The parallel component is represented by the minimum of the sine fit. The visiblity that was measured for particle three is -0.109 ± 0.003 and is plotted in Fig. 15. The intersection points are given in Tab. 2.

Intersection #	Particle three
1	a = 182.3 ± 0.2 nm
2	a = 335.5 ± 0.2 nm
3	a = 437.5 ± 0.2 nm
4	a = 591.4 ± 0.2 nm
5	a = 691.1 ± 0.2 nm
6	a = 847.2 ± 0.2 nm

Table 2: For the first six intersection points the radius that follows is presented.

To figure out the size of the particle we need to plot both the visibility of the Helium-Neon laser and the visiblity of the Diode laser in one figure, see Fig. 16. Both visibilities point to different possible particle sizes. For every intersection a vertical line is drawn. The blue vertical lines represent the radius that follows from the Diode laser measurement. The red vertical lines represent the radius that follows form the Helium-Neon measurement. The size of the particle is the one were a red and a blue vertical line overlap. There are several points where the red and the blue line almost overlap or partly overlap, that is for a radius of 588 nm and 847 nm. Based on the errors in both intersections it is more likely that the particle has a size of around 847 nm. The sizes of the other four particles are determined with the same analysis as for particle three. The data and the analysis of these four particles can be found in the Appendix. The sizes of the five particles are presented in Tab. 3.

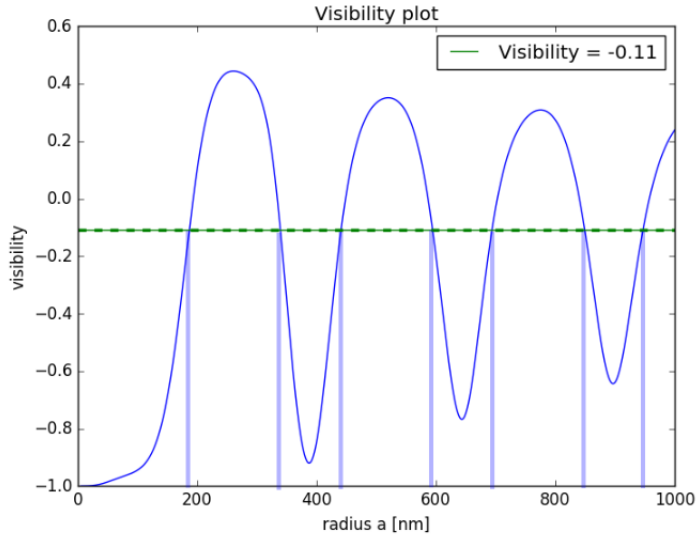

Figure 15: Visibility plot for particle three. The green line represents the measured value. The green dashed lines are the uncertainty in the visibility. The blue line is the simulation of the visibility for different particle sizes. The horizontal axis presents the radius in nm. The vertical axis displays the visibility.

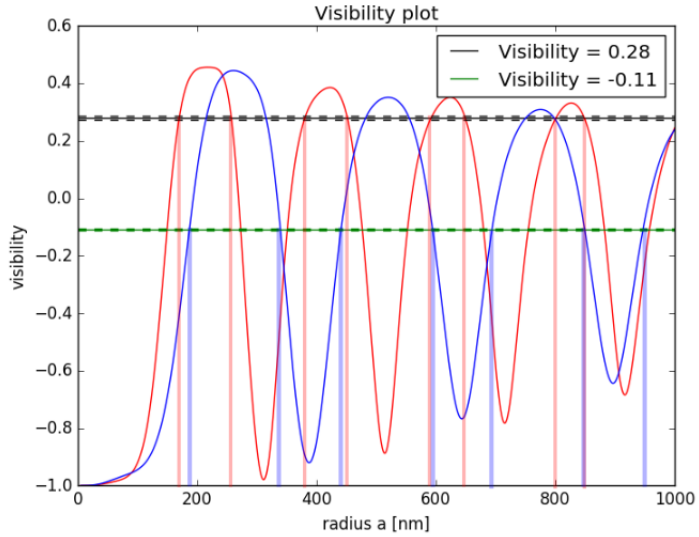

Figure 16: The black line represents the visiblity obtained with the Helium-Neon laser. The intersections of the black line with the red line point to the particles sizes determined with the Helium-Neon laser measurement. The green line represents the visiblity obtained with the Diode laser. The intersections of the green line with the blue line point to the particle sizes determind with the Diode laser measurement. The horizontal axis presents the radius in nm. The vertical axis displays the visibility.

Particle #	Particle size
1	a = 855 nm
2	a = 453 nm ± 1 nm
3	a = 846.5 nm ± 1 nm
4	a = 440 nm
5	a = 439.5 nm ± 2 nm

Table 3: For every particle the determined particle radius is presented.

5 Conclusion

We can say with certainty that the gold nano particles that are trapped in our linear Paul trap are not single colloids but aggregates. The radius of the injected spherical colloids is 50 nm. The radius of the trapped particles varies around 440 nm and 850 nm, see Tab. 3. This means the particles that we trapped are not proper to use for future research on laser ablation, for that we need single colloids.

The visibility that is calculated for the particles depends a lot on how the sine function fits to the scattering amplitude data points. The sine fit for the Diode laser data is very good. For the Helium-Neon laser data the sine function does not fit the data well for every particle. The data should be a perfect sine, and for the fact that it is not, there must be something wrong with the measurement with the Helium-Neon laser. For further research this problem should be solved first. Then the visibility could be calculated properly. If the visibility is calculated properly we expect that the visibility for particle one, two and four would change. The sine fit to these data sets is not good. The true visibility is probably a higher value for particle one and four, based on how the fit should be adjusted. With a higher visibility the intersection points for particle one and four would change in such a way that the determined particle radii will lie around 440 nm. For particle two the visibility is probably lower and the determined radius will lie around 450 nm.

For some particles there are several options for the particle size have a similar probability. Based on the intersection points that lie closest to eachother a conclusion is formed about the particle size. But the intersection points that lie closest to eachother are not very obvious. Something that would make it easier to determine the radius of the particles is to execute the experiment for another extra wavelength. In that case there will be three values for the visibility, which would make it easier to determine the true size of the particles, because there would be more intersections points that could be compared.

Based on the determined radii the particles have a diameter of bigger than 880 nm. In the experimental setup a filter for particles of 220 nm is placed. This tells us something about the place where these particles aggregate. Apparently the aggregation happens after the fluid passes the filter. For further research it is usefull in which part of the trapping process the particles aggregate. The concentration of particles in the solution could be determined before it enters a element of the setup. This concentration must then be compared with the concentration of the particles in the solution after it leaves an element of the setup. It can also be useful to research the effect of the dissolvent of the particles on the aggregation of the particles.

6 Appendix

In this section the results of the other four particles are presented. The same analysis was used for these particles as was used for particle three, which is described in the Results section.

6.1 Particle one

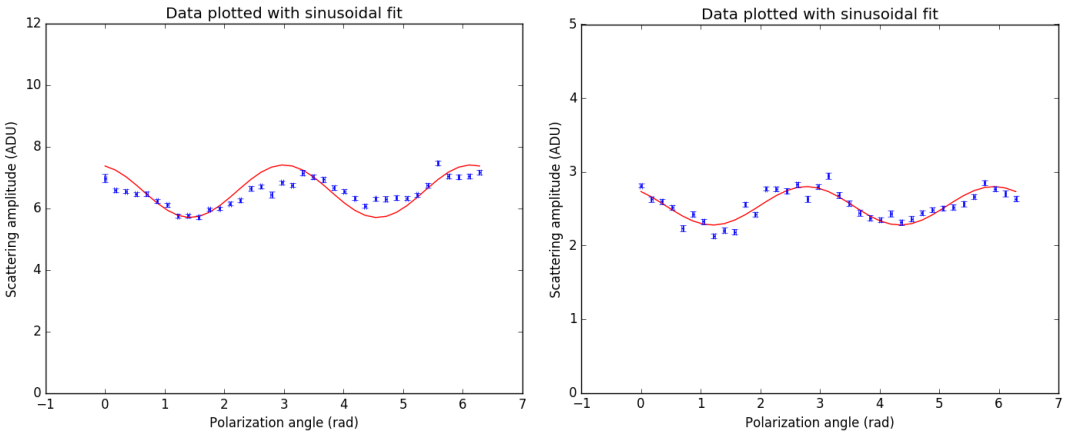

Figure 17: The left figure shows the scattering amplitude of the Helium-Neon measurement. The right figure shows the scattering amplitude of te Diode laser. The red line represents the sine fit through the data points. On the vertical axis the scattering amplitude is represented in analog to digital units. The horizontal axis displays the polarization angle.

For particle one it can be observed that the sine function is not fitted very well. This is reflected in the uncertainty of the visiblity. The visibility that is calculated for the Helium-Neon measurement is 0.130 ± 0.011. The visibility that is calculated for the Diode laser measurement is -0.103 ± 0.009. Both visibilities are plotted in Fig. 18. The intersection points that follow from these visibilities are presented in Tab. 4. For the intersections of the Helium-Neon laser scattering plots are made, see Fig. 19. From the scattering plots we can conclude the same thing as we did on particle three. The contrast between the sideway scattered light and the forward scattered light was quite big. The simulations for the particles with a smaller radius (156 and 266 nm) do not show this large contrast. Therefore the particles must be bigger than 266 nm. If we compare the intersection points found in our two measurements we can not determine the size of particle one correct. In Fig. 18 the red vertical lines represent the intersections for the Helium-Neon measurement. The blue vertical lines represent the intesections for the Diode laser. There is no point in this figure where the red and the blue vertical lines overlap or almost overlap. This means we should conclude that the intersection of the red and blue vertical lines lies outside the range of this graph. But from the scattering graphs we can derive that it is very unlikely that the particles are bigger than 1000 nm. The bigger the radius gets the more forward scattering there is. For a radius of 865 nm there is almost exclusively forward scattering. If the radius is even bigger than 1000 nm, the amount of sideways scattered light is very low. It was possible to observe the particles sideways when they were irradiated with the Helium-Neon laser. This makes it very unlikely that the particles are bigger than 1000 nm. It is more likely that the uncertainty in the visibility is underestimated. The sine fit is not very smooth trough the data points. If the uncertainty in the visiblity would be larger, the uncertainty in the radius will also be bigger. Based on how far the intersection points lie from eachother, it is most likely that particle one has a radius between 864.8 and 846.7 nm.

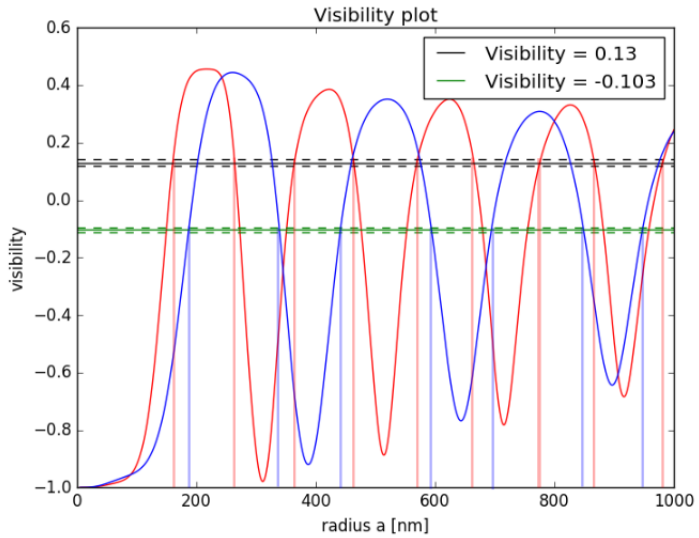

Figure 18: This figure shows both the visiblity for the Helium-Neon measurement as well as the visiblity of the Diode laser measurement. The black line represents the visiblity of the Helium-Neon measurement. The red line is the simulation of the visibility for different particle sizes for a wavelength of 633 nm. The light red vertical lines are drawn to clarify the intersection points of the Helium-Neon measurement. The green line shows the visibility that was measured for the Diode laser. The green dashed lines show the uncertainty in this visiblity. The blue line is the simulation of the visiblity for different particle sizes for a wavelenght of 785 nm. The light blue vertical lines are drawn to clarify the interscetion points that follow from the Diode measurement.

Intersection #	Helium-Neon	Diode
1	a = 155.8 ± 0.6 nm	a = 182.7 ± 0.5 nm
2	a = 260.1 ± 0.5 nm	a = 335.2 ± 0.4 nm
3	a = 360.5 ± 0.9 nm	a = 438.0 ± 0.6 nm
4	a = 460.4 ± 0.7 nm	a = 591.0 ± 0.5 nm
5	a = 566.3 ± 1.1 nm	a = 691.6 ± 0.6 nm
6	a = 662.3 ± 0.9 nm	a = 846.7 ± 0.7 nm
7	a = 773.0 ± 1.3 nm	
8	a = 864.8 ± 1.0 nm	

Table 4: For both the Helium-Neon measurement and the Diode laser the intersections points are presented.

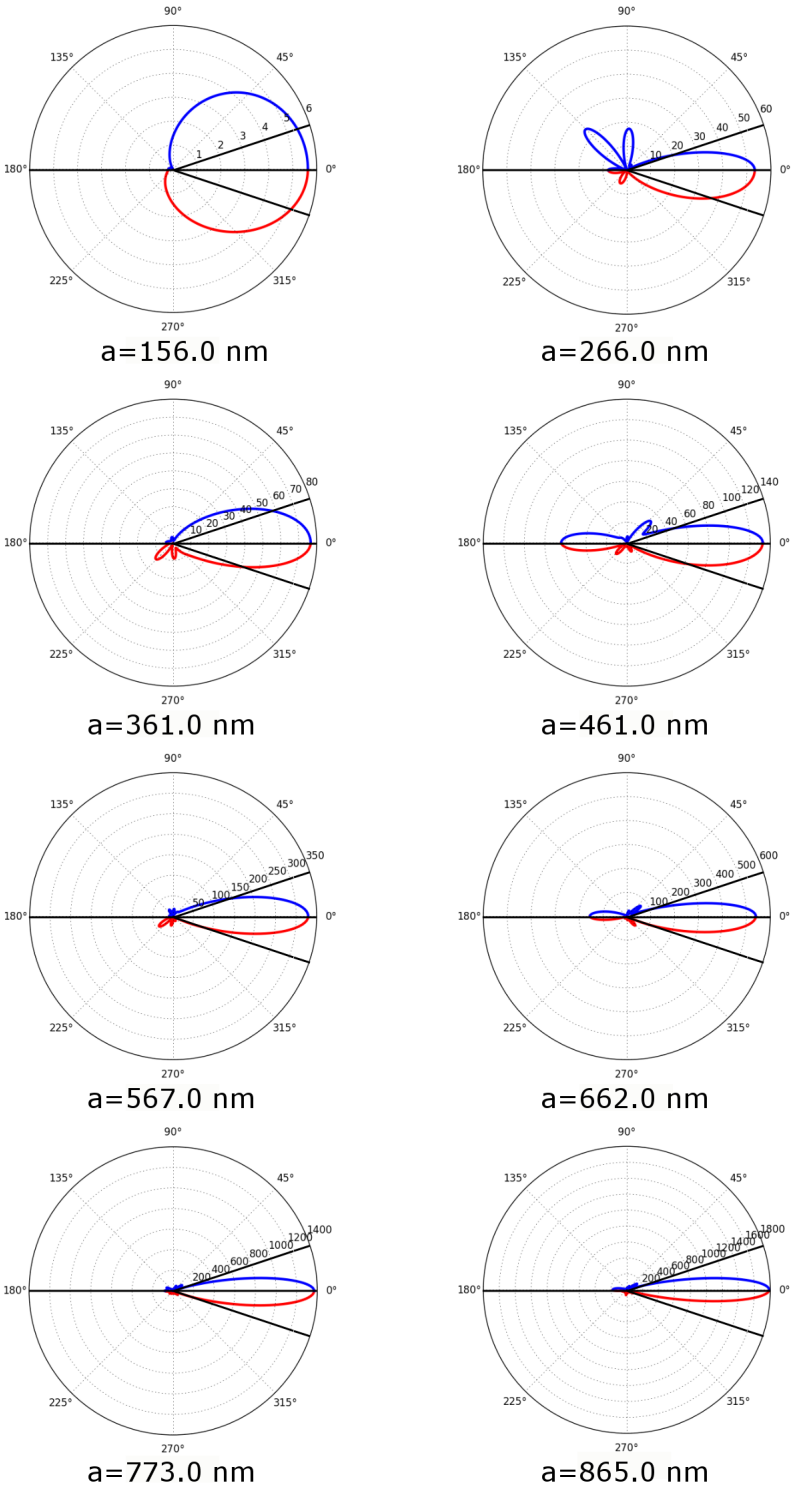

Figure 19: Simulation of the scattering of eight possible particles sizes for particle one, measured for the Helium-Neon laser. In each graph the parallel (blue) and perpendicular (red) component are shown. Here 0° degrees represents the forward direction, 180° the backward direction. In the r-axis the scattering amplitude is displayed. The two black oblique lines represent an angle of 20 degrees. The particles were observed at this angle to obtain information about the intensity of the forward scattered light. For more information about how this figure was established, see Fig. 5.

6.2 Particle two

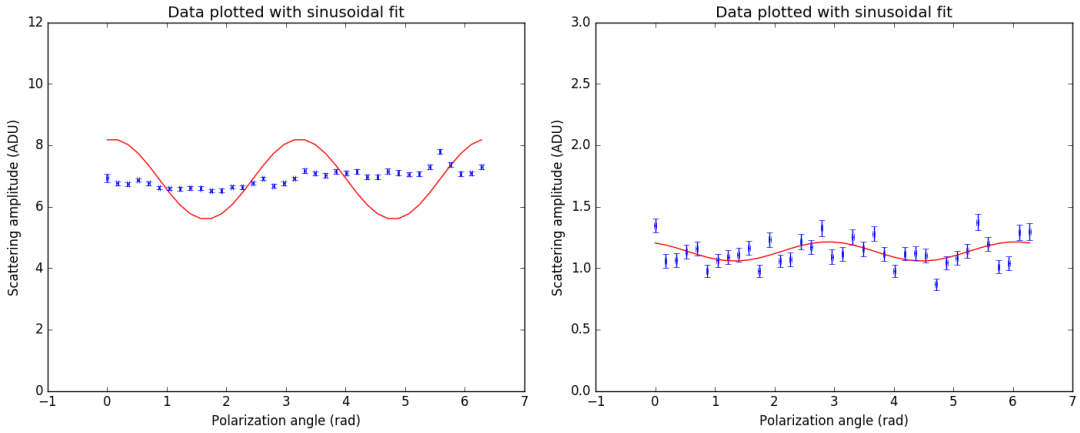

Figure 20: The left figure shows the scattering amplitude of the Helium-Neon measurement. The right figure shows the scattering amplitude of te Diode laser. The red line represents the sine fit through the data points. On the vertical axis the scattering amplitude is represented in analog to digital units. The horizontal axis displays the polarization angle.

For the Helium-Neon measurement the sine function did not fit the data. The visibility that was calculated for this measurement is 0.186 ± 0.120. The visibility calculated for the Diode laser is -0.068 ± 0.020, see Fig. 21. The visibility calculated from the sine fit for the Helium-Neon measurement is too incorrect to use. The true visibility would lie closer around 0. There is a small maximum visible for the first measured angle. For the Helium-Neon measurement the parallel component is represented by the maximum in the sine fit. According to Eq. 25 the visibility should have a positive value. A guess was made that the visibility should lie around 0.05 ± 0.08. The intersections that follows from these visibilities are presented in Tab. 5. For the first eight intersections of the Helium-Neon laser measurement a scattering plot is made. On the basis of these scattering plots we can conclude that the particles have a radius bigger than 263 nm. This was concluded in the same way as for particle three. In Fig. 21 the intersection points are clarified with red and blue vertical lines. The red lines do not overlap with the blue lines. This gives us the same problem as for particle one. Based on the same arguments as for particles one it is unlikely that the particles are bigger than 1000 nm. Thus the guess that was made for the visibility for the Helium-Neon measurement was wrong. Probably the visibility lies even closer to zero than we had taken into account. Another thing that can be noticed is that the data for the Diode laser looks also very different than for the other four particles. The data points have a much bigger uncertainty in the y direction. This higher uncertainty is also represented in the uncertainty in the visibility, it is twice as big as for the other particles for the Diode laser measurement. If the visibility for the Helium-Neon measurement would be closer to zero some intersection points will lie closer to eachother. The most likely radius for particle two will then be between 440.1 and 465.2 nm.

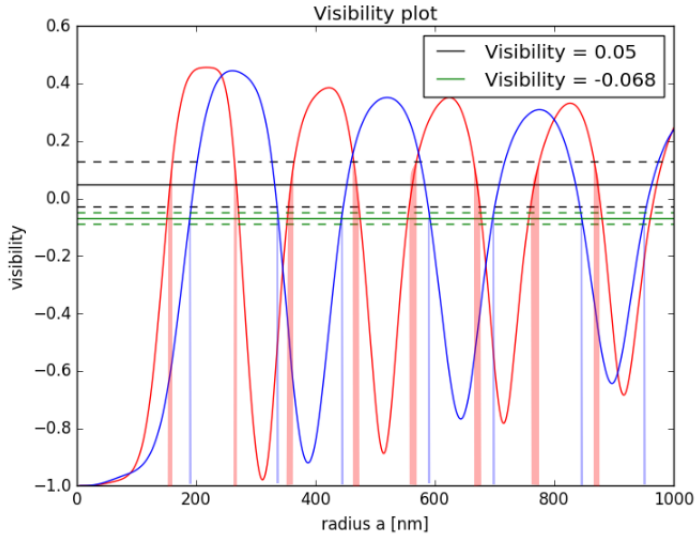

Figure 21: This figure shows both the visiblity for the Helium-Neon measurement as well as the visiblity of the Diode laser measurement. The black line represents the visiblity of the Helium-Neon measurement. The red line is the simulation of the visibility for different particle sizes for a wavelength of 633 nm. The light red vertical lines are drawn to clarify the intersection points of the Helium-Neon measurement. The green line shows the visibility that was measured for the Diode laser. The green dashed lines show the uncertainty in this visiblity. The blue line is the simulation of the visiblity for different particle sizes for a wavelenght of 785 nm. The light blue vertical lines are drawn to clarify the interscetion points that follow from the Diode measurement

Intersection #	Helium-Neon	Diode
1	a = 151.8 ± 3.7 nm	a = 184.7 ± 1.2 nm
2	a = 263.2 ± 3.0 nm	a = 333.5 ± 1.0 nm
3	a = 355.1 ± 4.6 nm	a = 440.1 ± 1.4 nm
4	a = 465.2 ± 4.6 nm	a = 588.6 ± 1.5 nm
5	a = 559.3 ± 6.3 nm	a = 694.3 ± 1.7 nm
6	a = 668.0 ± 5.3 nm	a = 844.0 ± 1.8 nm
7	a = 764.4 ± 6.8 nm	a = 948.8 ± 2.0 nm
8	a = 870.9 ± 5.6 nm	
9	a = 970.2 ± 8.3 nm	

Table 5: For both the Helium-Neon measurement and the Diode laser the intersections points are presented.

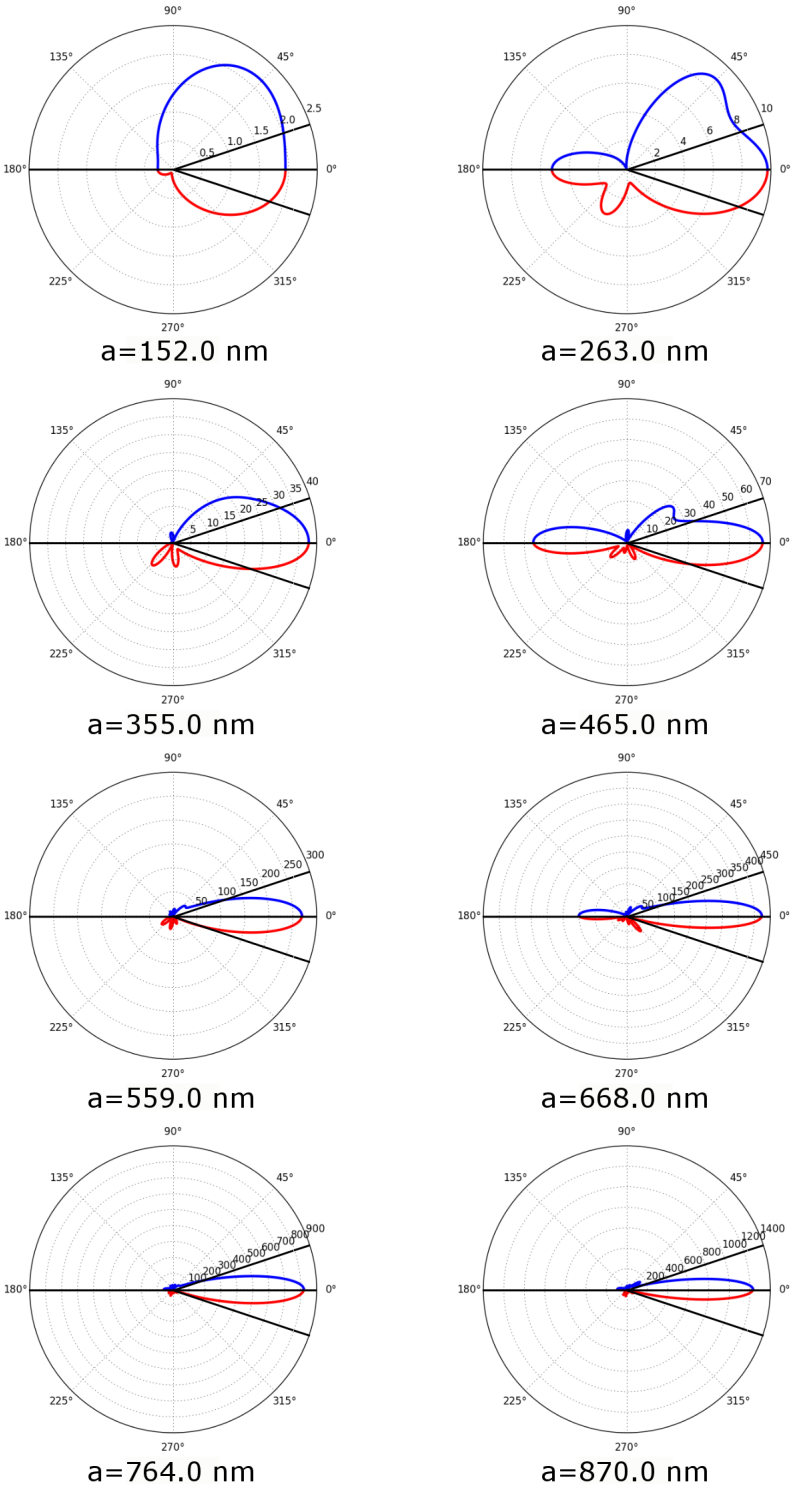

Figure 22: Simulation of the scattering of eight possible particles sizes for particle three, measured for the Helium-Neon laser. In each graph the parallel (blue) and perpendicular (red) component are shown. Here 0° degrees represents the forward direction, 180° the backward direction. In the r-axis the scattering amplitude is displayed. The two black oblique lines represent an angle of 20 degrees. The particles were observed at this angle to obtain information about the intensity of the forward scattered light. For more information about how this figure was established, see Fig. 5.

6.3 Particle four

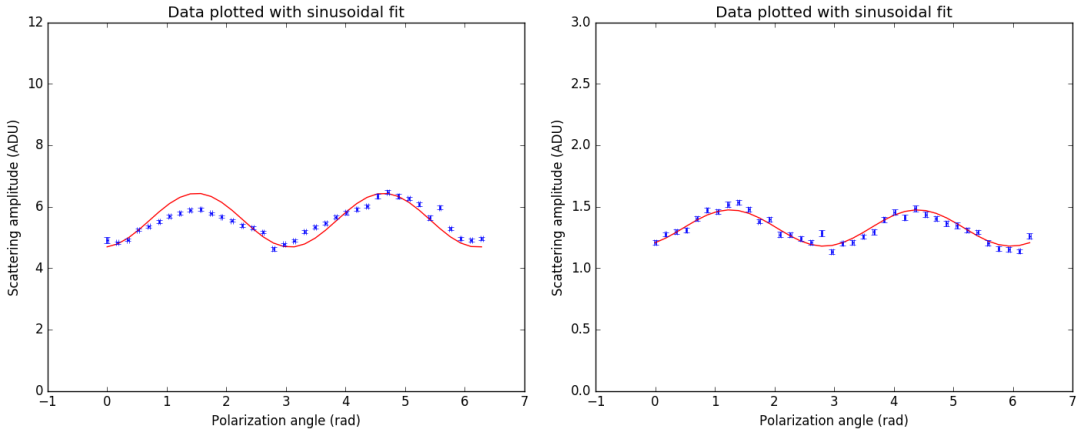

Figure 23: The left figure shows the scattering amplitude of the Helium-Neon measurement. The right figure shows the scattering amplitude of te Diode laser. The red line represents the sine fit through the data points. On the vertical axis the scattering amplitude is represented in analog to digital units. The horizontal axis displays the polarization angle.

For particle four the sine fit for the Helium-Neon measurement is also not very well. It seems like the amplitude of the data becomes higher for bigger polarization angles. The sine function can therefore not make a good fit to the data. The visibility for the Helium-Neon laser is -0.156 ± 0.008. The visibility for the Diode laser is 0.111 ± 0.007. The visibilities are plotted in Fig. 24. For particle number four the sine fit displays a minimum first instead of a maximum. The visibility for the Helium-Neon measurement is therefore a negative number instead of a positive number. The other four particles do have a positive visiblity for the Helium-Neon measurement. The visibility for the Diode laser measurement is positive instead of negative. The intersection points that follow from these visibilities are presented in Tab. 5. For the first eight intersections of the Helium-Neon measurement scattering plots are made, see Fig. 25. The contrast between the sideway scattered light and the forward scattered light for the Helium-Neon laser was big. In the scattering plots the first three possible particle radii show a small contrast. The radius of particle four must be bigger than 270 nm. In Fig. 24 there is no overlap between a red vertical line and a blue vertical line. Just as for particle one we should conclude that the intersection must lie outside the range of this graph. But again based on the scattering graphs it is unlikely that the particles have a bigger radius than 1000 nm. Probably the uncertainty in the Helium-Neon measurement is undersetimated again. The uncertainty in the visibility for the Helium-Neon measurement is now a bit bigger than the uncertainty for the Diode laser measurement. But if we compare the two sine fits in Fig. 23, the fit for the Helium-Neon measurement is obviously a lot worse than the one for the Diode laser measurement. Therefore the uncertainty in the visibility for the Helium-Neon measurement is probably underestimated. If the uncertainty will be bigger it is most likely the radius of particle four lies between 454.4 and 437.3 nm.

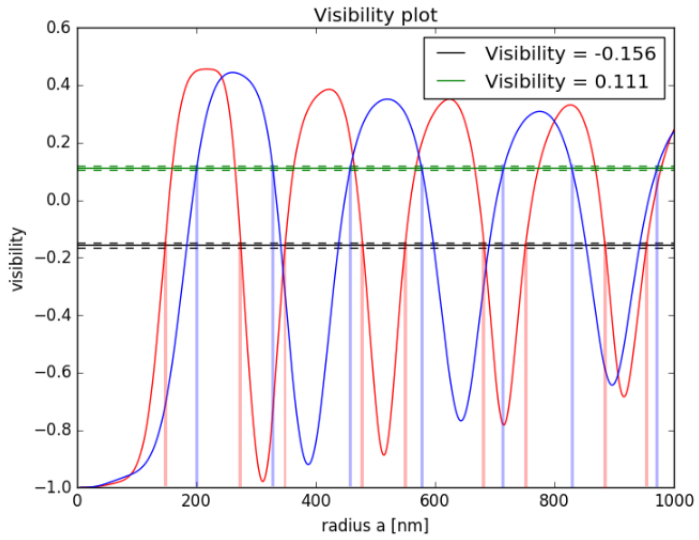

Figure 24: This figure shows both the visiblity for the Helium-Neon measurement as well as the visiblity of the Diode laser measurement. The black line represents the visiblity of the Helium-Neon measurement. The red line is the simulation of the visibility for different particle sizes for a wavelength of 633 nm. The light red vertical lines are drawn to clarify the intersection points of the Helium-Neon measurement. The green line shows the visibility that was measured for the Diode laser. The green dashed lines show the uncertainty in this visiblity. The blue line is the simulation of the visiblity for different particle sizes for a wavelenght of 785 nm. The light blue vertical lines are drawn to clarify the interscetion points that follow from the Diode measurement.

Intersection #	Helium-Neon	Diode
1	a = 142.9 ± 0.3 nm	a = 196.3 ± 0.5 nm
2	a = 270.2 ± 0.2 nm	a = 324.2 ± 0.4 nm
3	a = 344.9 ± 0.3 nm	a = 454.4 ± 0.7 nm
4	a = 473.3 ± 0.4 nm	a = 574.4 ± 0.6 nm
5	a = 546.7 ± 0.4 nm	a = 712.3 ± 0.8 nm
6	a = 679.3 ± 0.3 nm	a = 826.9 ± 0.9 nm
7	a = 749.2 ± 0.5 nm	a = 970.2 ± 1.1 nm
8	a = 882.7 ± 0.4 nm	
9	a = 952.7 ± 0.6 nm	

Table 6: For both the Helium-Neon measurement and the Diode laser the intersections points are presented.

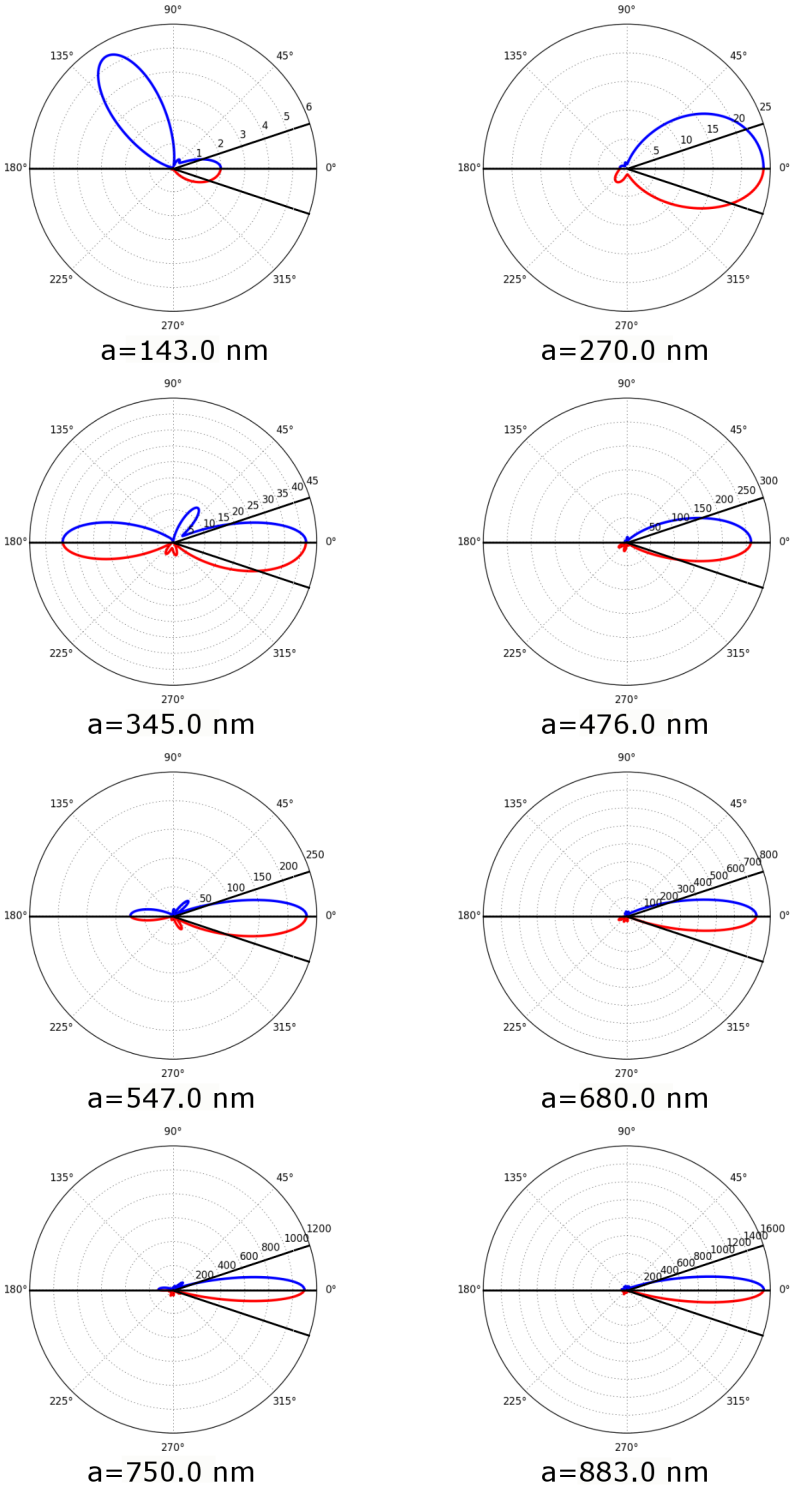

Figure 25: Simulation of the scattering of eight possible particles sizes for particle four, measured for the Helium-Neon laser. In each graph the parallel (blue) and perpendicular (red) component are shown. Here 0° degrees represents the forward direction, 180° the backward direction. In the r-axis the scattering amplitude is displayed. The two black oblique lines represent an angle of 20 degrees. The particles were observed at this angle to obtain information about the intensity of the forward scattered light. For more information about how this figure was established, see Fig. 5.

6.4 Particle five

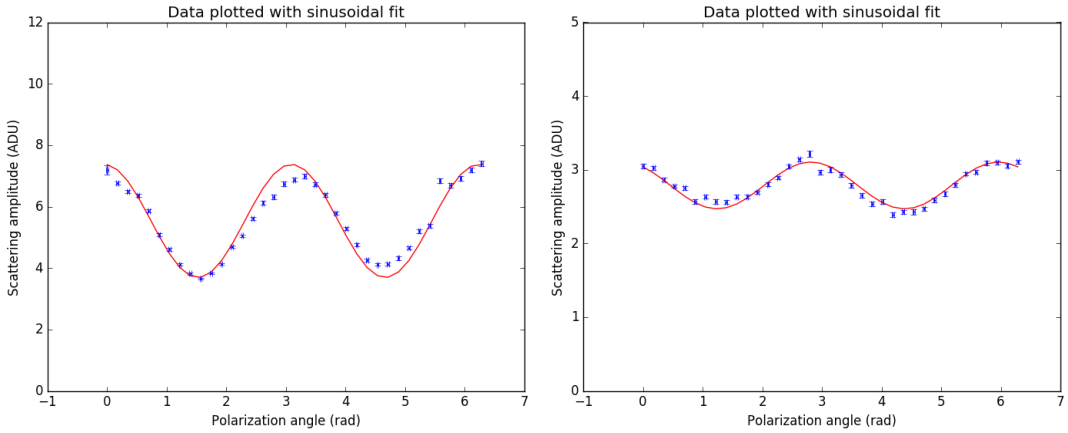

Figure 26: The left figure shows the scattering amplitude of the Helium-Neon measurement. The right figure shows the scattering amplitude of te Diode laser. The red line represents the sine fit through the data points. On the vertical axis the scattering amplitude is represented in analog to digital units. The horizontal axis displays the polarization angle.

The visibilty measured with the Helium-Neon laser is 0.323 ± 0.060. The visibility measured with the Diode laser is -0.114 ± 0.006. These visibilities are used to create Fig. 27. The intersection points that follow from these intersections are presented in Tab. 6. For the first eight intersection points that follow from the Helium-Neon measurement a scattering plot is made, see Fig. 28. On the basis of these scattering plots we conclude that the particles have a bigger radius than 250 nm. This is concluded in the same way as for the other four particles. The light red lines in Fig. 27 almost overlap with the light blue lines. This points to a radius of approximately 440 nm for particle five.

Intersection #	Helium-Neon	Diode
1	a = 169.1 ± 0.6 nm	a = 182.1 ± 0.3 nm
2	a = 250.2 ± 0.5 nm	a = 335.7 ± 0.2 nm
3	a = 385.3 ± 1.5 nm	a = 437.2 ± 0.3 nm
4	a = 442.3 ± 0.9 nm	a = 591.7 ± 0.4 nm
5	a = 601.5 ± 2.1 nm	a = 690.8 ± 0.4 nm
6	a = 637.6 ± 1.8 nm	a = 847.5 ± 0.4 nm
7	a = 814.6 ± 2.2 nm	
8	a = 834.1 ± 3.5 nm	

Table 7: For both the Helium-Neon measurement and the Diode laser the intersections points are presented.

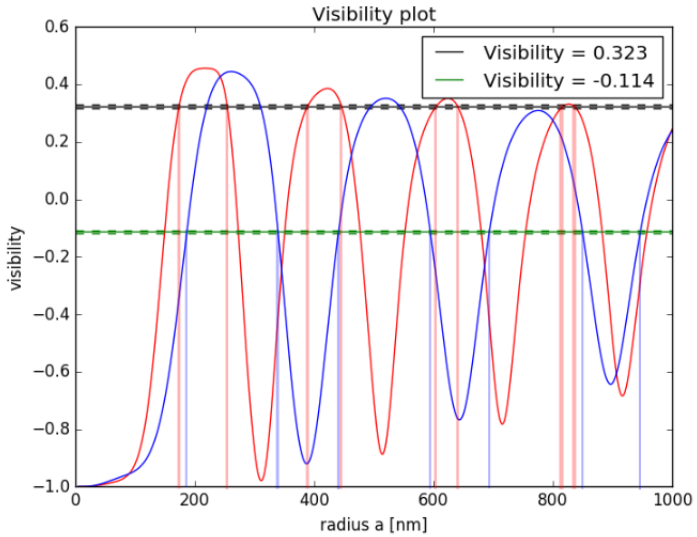

Figure 27: This figure shows both the visiblity for the Helium-Neon measurement as well as the visiblity of the Diode laser measurement. The black line represents the visiblity of the Helium-Neon measurement. The red line is the simulation of the visibility for different particle sizes for a wavelength of 633 nm. The light red vertical lines are drawn to clarify the intersection points of the Helium-Neon measurement. The green line shows the visibility that was measured for the Diode laser. The green dashed lines show the uncertainty in this visiblity. The blue line is the simulation of the visiblity for different particle sizes for a wavelenght of 785 nm. The light blue vertical lines are drawn to clarify the interscetion points that follow from the Diode measurement.

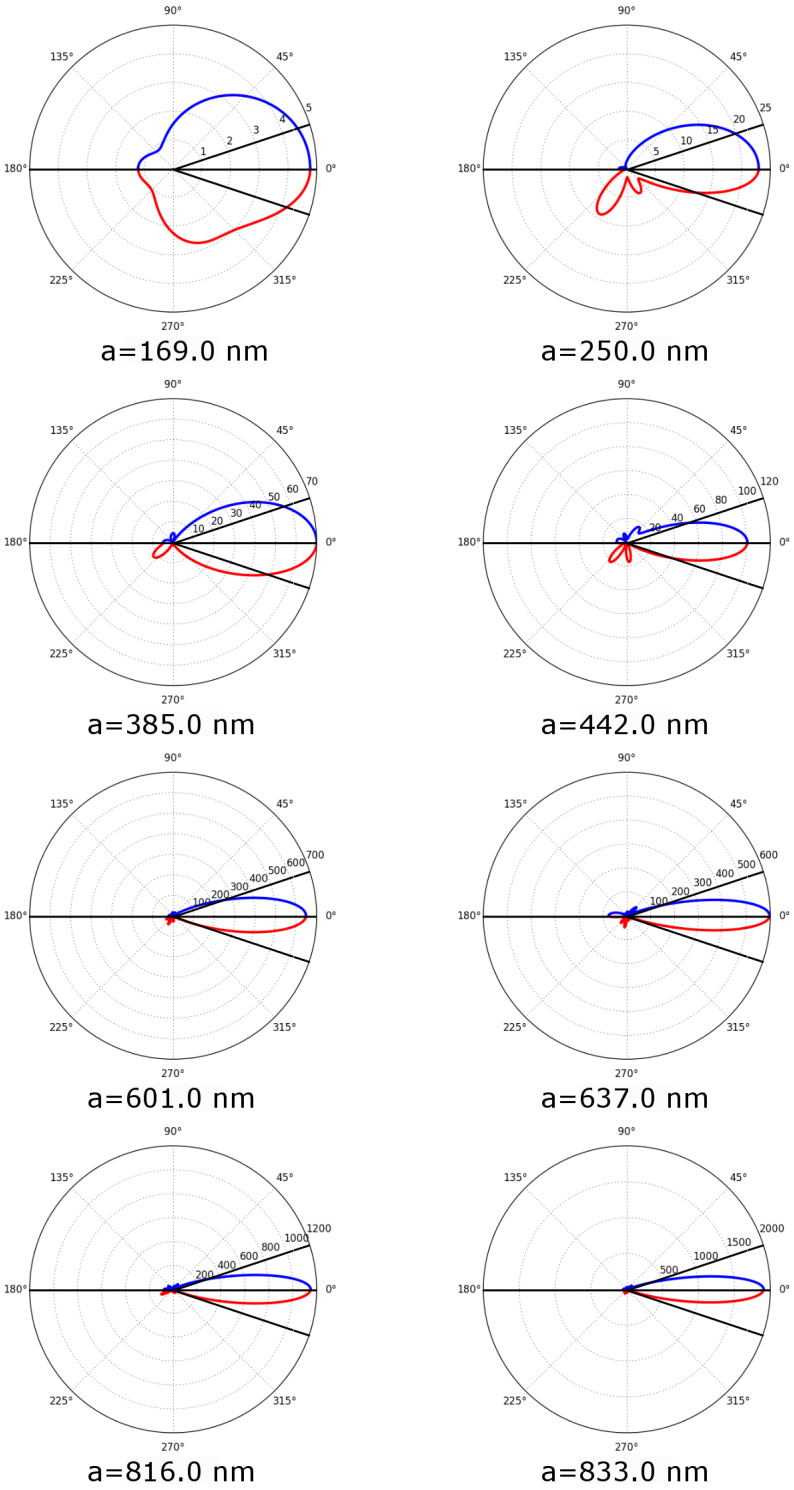

Figure 28: Simulation of the scattering of eight possible particles sizes for particle five, measured for the Helium-Neon laser. In each graph the parallel (blue) and perpendicular (red) component are shown. Here 0° degrees represents the forward direction, 180° the backward direction. In the r-axis the scattering amplitude is displayed. The two black oblique lines represent an angle of 20 degrees. The particles were observed at this angle to obtain information about the intensity of the forward scattered light. For more information about how this figure was established, see Fig. 5.

References

[1] Nobelprize.org, "The nobel prize in physics 1989." Nobel Media AB.

[2] W. Paul, "Electromagnetic traps for charged and neutral particles," *Reviews of modern physics*, vol. 62, no. 3, p. 531, 1990.

[3] K. L. Kelly, E. Coronado, L. L. Zhao, and G. C. Schatz, "The optical properties of metal nanoparticles: the influence of size, shape, and dielectric environment," *The Journal of Physical Chemistry B*, vol. 107, no. 3, pp. 668–677, 2003.

[4] L. Ruby, "Applications of the mathieu equation," *American Journal of Physics*, vol. 64, no. 1, pp. 39–44, 1996.

[5] D. Douglas, "Linear quadrupoles in mass spectrometry," *Mass spectrometry reviews*, vol. 28, no. 6, pp. 937–960, 2009.

[6] C. F. Bohren and D. R. Huffman, *Absorption and scattering of light by small particles*. John Wiley & Sons, 2008.

[7] H. C. Hulst and H. Van De Hulst, *Light scattering by small particles*. Courier Corporation, 1957.

[8] J. Leinonen, "Pymiecoated." MIT license, 10 2012.